GASTROINTESTINAL DISEASE

Cognitive impairments induced by necrotizing enterocolitis can be prevented by inhibiting microglial activation in mouse brain

Diego F. Niño[1,2], Qinjie Zhou[1,2], Yukihiro Yamaguchi[1,2], Laura Y. Martin[1,2], Sanxia Wang[1,2], William B. Fulton[1,2], Hongpeng Jia[1,2], Peng Lu[1,2], Thomas Prindle Jr.[1,2], Fan Zhang[3], Joshua Crawford[4], Zhipeng Hou[5], Susumu Mori[5], Liam L. Chen[6], Andrew Guajardo[6], Ali Fatemi[7], Mikhail Pletnikov[4,8], Rangaramanujam M. Kannan[9], Sujatha Kannan[10], Chhinder P. Sodhi[1,2]*, David J. Hackam[1,2]*

Necrotizing enterocolitis (NEC) is a severe gastrointestinal disease of the premature infant. One of the most important long-term complications observed in children who survive NEC early in life is the development of profound neurological impairments. However, the pathways leading to NEC-associated neurological impairments remain unknown, thus limiting the development of prevention strategies. We have recently shown that NEC development is dependent on the expression of the lipopolysaccharide receptor Toll-like receptor 4 (TLR4) on the intestinal epithelium, whose activation by bacteria in the newborn gut leads to mucosal inflammation. Here, we hypothesized that damage-induced production of TLR4 endogenous ligands in the intestine might lead to activation of microglial cells in the brain and promote cognitive impairments. We identified a gut-brain signaling axis in an NEC mouse model in which activation of intestinal TLR4 signaling led to release of high-mobility group box 1 in the intestine that, in turn, promoted microglial activation in the brain and neurological dysfunction. We further demonstrated that an orally administered dendrimer-based nanotherapeutic approach to targeting activated microglia could prevent NEC-associated neurological dysfunction in neonatal mice. These findings shed light on the molecular pathways leading to the development of NEC-associated brain injury, provide a rationale for early removal of diseased intestine in NEC, and indicate the potential of targeted therapies that protect the developing brain in the treatment of NEC in early childhood.

INTRODUCTION

Necrotizing enterocolitis (NEC) is the leading cause of death and disability from gastrointestinal disease in premature infants and is characterized by the sudden onset of patchy intestinal ischemia and necrosis (*1, 2*). About 10% of premature infants will develop NEC, and the total number of affected infants is slowly rising due, in part, to an increasing number of premature births (*3, 4*). Although the pathways leading to NEC remain incompletely understood, we (*5, 6*) and others (*7, 8*) have shown that the combination of formula feeds, brief hypoxic episodes, and activation of the lipopolysaccharide (LPS) receptor Toll-like receptor 4 (TLR4) on the intestinal epithelium, which is expressed at higher levels in premature as compared with full-term infants (*1, 6, 9*), are seen in a majority of cases in which NEC develops. Although the overall survival of infants after an episode of NEC is about 50% (*2*), in those children who do survive the initial disease, nearly half will develop profound neurological impairments (*10, 11*), which are both more severe and more difficult to treat than the brain injuries that develop in premature infants who do not develop NEC (*12–14*).

Using either the chronic hypoxia (*15*) or the carotid ligation models (*16*) of perinatal brain injury, previous investigators have shown that activation of microglia leads to an impairment of oligodendrocyte progenitor cells (OPCs) (*15, 17*), resulting in myelination impairment (*18*) and cognitive dysfunction (*17, 19*). NEC-associated brain injury is similarly characterized by dysmyelination and reduced brain volume (*11, 20, 21*), leading us to test whether microglial activation and a deficit in myelination may also play a role in NEC-associated brain injury. Prior experimental animal studies of brain injury in premature newborns lack direct clinical relevance to NEC, given their failure to incorporate the key features of this disease, including formula gavage, brief hypoxia episodes, and TLR4 signaling (*1*).

Here, we used an experimental mouse model that replicates the key clinical features of both NEC and NEC-associated brain injury to understand the mechanisms mediating the development of NEC-associated brain injury. Our results showed that the intestinal injury in NEC leads to activation of TLR4 on microglial cells in the brain, resulting in the accumulation of reactive oxygen species (ROS), loss of OPCs, dysmyelination, and cognitive impairments. We further showed that, in NEC, the endogenous TLR4 ligand high-mobility

[1]Division of General Pediatric Surgery, Johns Hopkins University and Bloomberg Children's Center, Johns Hopkins Hospital, Baltimore, MD 21287, USA. [2]Division of General Pediatric Surgery, Johns Hopkins University and Johns Hopkins Children's Center, Johns Hopkins Hospital, Baltimore, MD 21287, USA. [3]Program of Immunology, Clinical Research Division, Fred Hutchinson Cancer Research Center, Seattle, WA 98109, USA. [4]Department of Psychiatry and Behavioral Sciences, Johns Hopkins School of Medicine, Baltimore, MD 21205, USA. [5]Department of Biomedical Engineering and The Russell H. Morgan Department of Radiology and Radiological Science, Johns Hopkins School of Medicine, Baltimore, MD 21205, USA. [6]Division of Neuropathology, Department of Pathology, Johns Hopkins School of Medicine, Baltimore, MD 21205, USA. [7]Departments of Neurology and Pediatrics, Kennedy Krieger Institute and Johns Hopkins University School of Medicine, MD 21205, USA. [8]Department of Molecular and Comparative Pathobiology and Solomon H. Snyder Department of Neuroscience, Johns Hopkins University and Johns Hopkins Children's Center, Johns Hopkins Hospital, Baltimore, MD 21205, USA. [9]Center for Nanomedicine, Wilmer Eye Institute, Department of Ophthalmology, Johns Hopkins University School of Medicine, Baltimore, MD 21287, USA. [10]Department of Anesthesiology and Critical Care Medicine, Johns Hopkins University School of Medicine, Baltimore, MD 21205, USA. *Corresponding author. Email: dhackam1@jhmi.edu (D.J.H.); csodhi@jhmi.edu (C.P.S.)

group box 1 (HMGB1) is released from the intestinal epithelium and activates brain microglia. Mice lacking HMGB1 on the intestinal epithelium subjected to NEC are protected from brain injury. The oral administration of a dendrimer nanoparticle coupled with the antioxidant agent *N*-acetyl-L-cysteine (NAC) substantially reduced OPC loss and prevented the detrimental neurocognitive effects of NEC. Together, these findings shed light on the molecular pathways leading to the development of NEC-associated brain injury and raise the possibility that targeted therapies that protect the developing brain may offer new hope for children who develop NEC in early childhood.

RESULTS

Experimental NEC leads to impaired myelination and cognitive dysfunction

To determine the pathogenesis of NEC-associated brain injury, we first subjected newborn mice to a mouse model of NEC using a combination of formula feeds, hypoxia, and the administration of stool from a child who had developed severe NEC (*6, 22–24*). To determine bacterial gene composition, the 16*S* ribosomal RNA pyrosequencing analysis of the stool from a patient with NEC is shown in table S1. As shown in fig. S1, this experimental approach induced marked disruption of the intestinal villus architecture, which resembles that seen in human NEC (fig. S1, A and B), and increased expression of the proinflammatory cytokine interleukin-1β (*Il-1*β) in the intestinal epithelium in both mouse and human intestine (fig. S1, C and D) (*1, 2*). The induction of NEC in mice also caused marked changes in the mouse brain 11 days postnatal (P11), characterized by reduced expression of myelin basic protein (Mbp) in the midbrain, the corpus callosum, and the rostroventral structures (Fig. 1A). Impaired myelination within the subcortical white matter of the temporal and frontal lobes was also observed in the brains of human infants with NEC (Fig. 1A), supporting the validity of the animal model (*11, 21*). A detailed histological analysis of the brains of infants with and without NEC is shown in fig. S2. The impairment of myelination in the mouse model of NEC was also observed by electron microscopy (EM) (Fig. 1, B and C) showing a reduction of myelin g-ratio compared to non-NEC controls (*25, 26*). Brain magnetic resonance imaging (MRI) evaluation was performed in a mouse model of NEC (Fig. 1D), which revealed a significant ($P \leq 0.0001$) reduction in overall total brain volume (Fig. 1, D and E) (*27*), which mirrors that seen in infants with NEC-associated brain injury (*11, 20, 21*). Neuronal density as determined by immunostaining for neuronal nuclei (NeuN) was similar between groups (Fig. 1, F and G). These results, in combination with the EM findings, suggest that a loss of neurons or axons does not account for the loss of myelin reported in the brain of NEC animals.

Given the fact that other experimental models of perinatal brain injury have exposed mice to episodic hypoxia (*28*), we assessed the degree of myelination in the brains of mice that were exposed to the same hypoxia treatment alone that was used in our experimental NEC protocol (5% O_2, 10 min twice daily for 4 days) and found that the exposure to hypoxia alone had no effect on the pattern of staining of Mbp in the mouse brain (fig. S3, A and B) or on brain volume (fig. S3C).

We next explored the effects of NEC on neurocognitive function in the brains of mice that had reached 7 to 12 weeks of age and that had been exposed to 3 days of the model earlier in life. As shown in Fig. 1 (H and I), exposure of 7-day-old mice to experimental NEC resulted in severe cognitive deficits when mice reached maturity, as evidenced by significantly impaired ($P \leq 0.001$) spatial working memory (Fig. 1H) and novel object recognition memory (Fig. 1I) (*29*). These abnormalities in neurocognitive performance in mice resemble the impaired learning and memory reported in human infants who survive NEC (*30*), providing further validity of the current animal model. Together, these findings showed that experimental NEC leads to a myelination deficit and cognitive impairments that resemble the neurodevelopmental deficits observed in infants. We next sought to determine the mechanisms involved and to devise a strategy to prevent them.

NEC leads to TLR4-dependent microglial activation and loss of OPCs

We next focused on whether microglial activation could play a role in the reduced myelin deposition that we observed in the brains of mice and humans with NEC. As shown in Fig. 2A, we observed a significant increase in the expression of the microglial marker ionized calcium-binding adaptor molecule 1 (Iba-1) in the brains of human infants with NEC as compared with control brains [control, 198.8 ± 27 ($n = 5$) versus NEC, 549 ± 82 ($n = 5$); $P < 0.01$], indicating that microglial activation accompanies the development of NEC-associated brain injury. We also noted an increase in Iba-1 staining in the whole-brain sagittal sections obtained from a mouse model of NEC as compared with age-matched breastfed control mice, which was seen predominantly within the regions of the hippocampus, the periventricular area, and the midbrain (Fig. 2B and quantified in Fig. 2E). Other markers of inflammatory signaling were observed in the brains of a mouse model of NEC, including increased accumulation of ROS, as revealed by dihydroethidium (DHE) staining (Fig. 2C and quantified in Fig. 2F), which was detected in areas where we also saw reduced expression of Mbp (Fig 2D and quantified in Fig. 2G). NEC induction in oligodendrocyte lineage reporter $Pdgfr\alpha^{GFP}$ showed that the activation of microglia in NEC-induced brain injury was associated with a loss of OPCs, as revealed by reduced expression of green fluorescent protein (GFP) (Fig. 2H and quantified in Fig. 2I). These findings were not associated with changes in neuronal density within the hippocampus, as shown above.

To evaluate the role that the stool microbiota used to induce NEC plays in our model, a control group of mice was submitted to the same experimental protocol used to induce NEC, except that we replaced the bacterial component with bacteria isolated from a healthy infant (16*S* analysis of the bacterial composition of the stool from an NEC patient and stool from a control patient is shown in tables S1 and S2) (*31*). As depicted in fig. S4, the use of bacteria isolated from a healthy infant to supplement the formula feeding did not lead to intestinal injury resembling NEC (fig. S4, A and B) and did not cause any brain injury (fig. S4, C to H).

To determine the potential upstream pathways that could mediate microglial activation in the pathogenesis of NEC-associated brain injury, we next focused on the observation that, in other experimental models, microglial activation is mediated in part by TLR4, whose ligands include bacterial LPS and various endogenous molecules (*32, 33*). To determine whether TLR4 signaling leads to microglial activation in NEC-associated brain injury, we next generated mice lacking TLR4 in the microglia ($TLR4^{\Delta Cx3cr1}$) and subjected these animals to experimental NEC. The generation and confirmation of the $TLR4^{\Delta Cx3cr1}$ mice are shown in fig. S5, in which the detection of

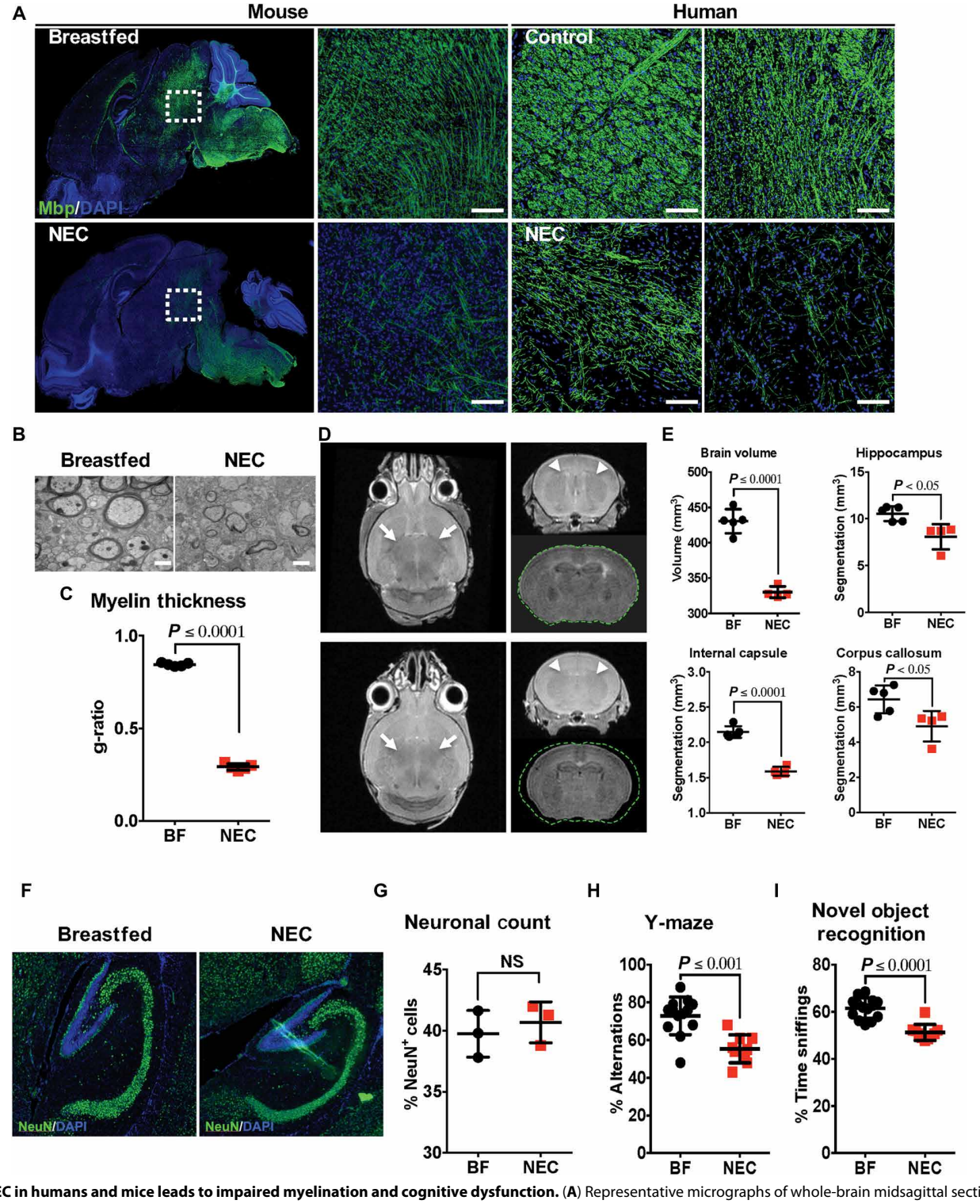

Fig. 1. NEC in humans and mice leads to impaired myelination and cognitive dysfunction. (**A**) Representative micrographs of whole-brain midsagittal sections from P11 mice or preterm humans with NEC or controls [breastfed (BF)] stained for Mbp. Scale bars, 50 μm. DAPI, 4′,6-diamidino-2-phenylindole. (**B**) Representative transmission EM images of midbrain sections from a mouse model of NEC in P11 mice or breastfed controls. Scale bars, 2 μm. (**C**) Myelin g-ratio (myelin sheath thickness; calculated as axon diameter/axon diameter with myelin) in the midbrain region obtained from a mouse model of NEC in P11 mice or breastfed controls ($n = 5$ per experimental group). (**D**) Representative horizontal and coronal T2-weighted images from P11 mice; white arrows indicate internal capsule, and arrowheads indicate corpus callosum/external capsule. (**E**) Volumetric and segmentation analysis of T2-weighted images from P11 mice; means ± SD ($n = 5$ breastfed controls and $n = 4$ NEC). (**F**) Representative confocal micrographs of the hippocampus (midsagittal section) from a mouse model of NEC in P11 mice or breastfed controls stained for NeuN; quantification in (**G**) ($n = 3$ per experimental group). NS, not significant. (**H** and **I**) Cognitive evaluation by Y-maze (H) and novel object recognition (I) ($n = 13$ breastfed controls and $n = 9$ NEC). Experiments were performed in triplicate with at least three mice per group per experiment. Statistical differences were determined using Student's *t* test.

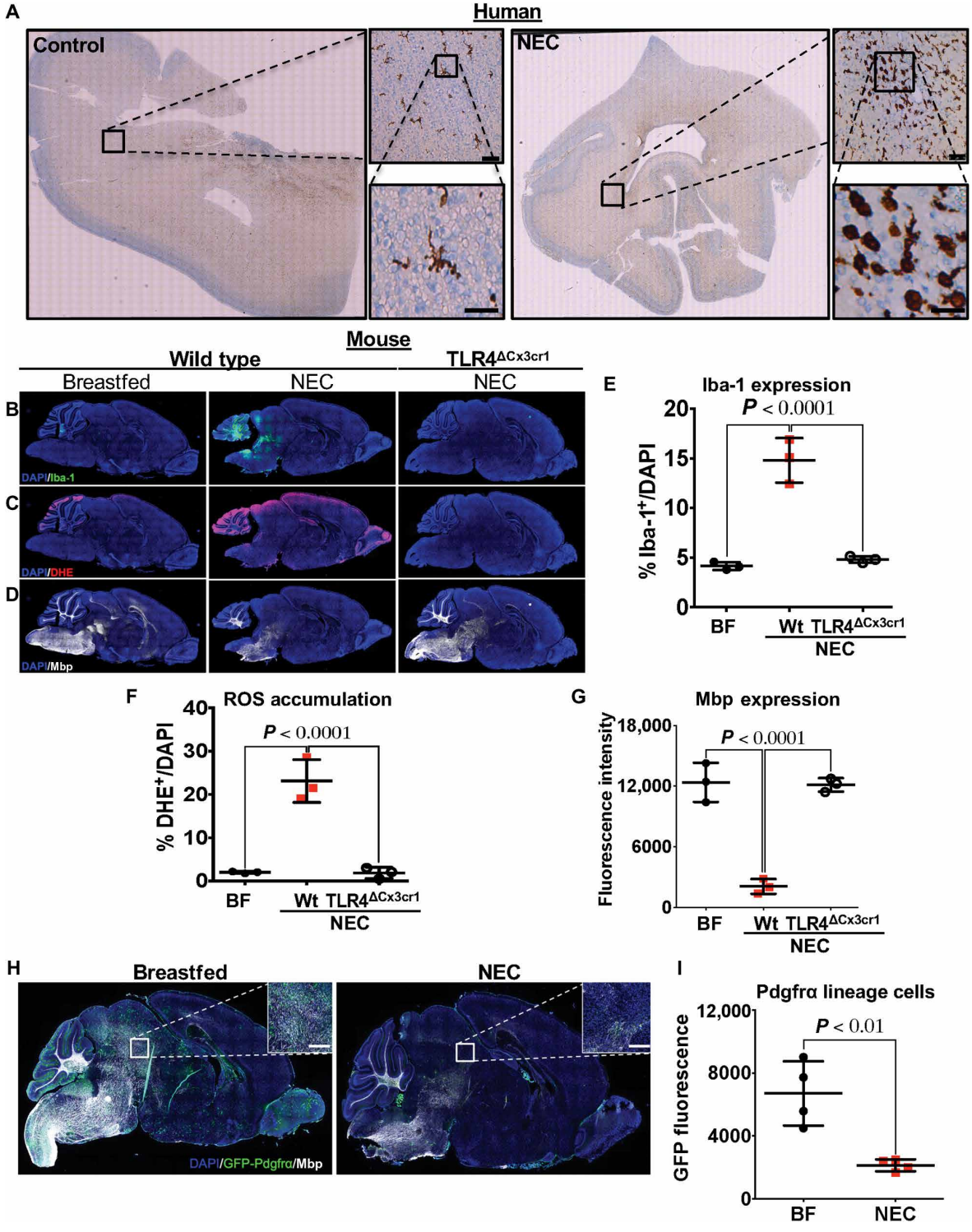

Fig. 2. NEC leads to TLR4-dependent microglial activation and loss of OPCs in the newborn brain. (**A**) Representative micrographs of Iba-1 3,3′-diaminobenzidine immunostaining of periventricular brain sections obtained from autopsy specimens of premature human infants with NEC or controls ($n = 5$ per group). Scale bars, 75 μm (top) and 25 μm (bottom). (**B** to **G**) Representative staining (B to D) and quantification (E to G) as indicated in whole-brain midsagittal sections from wild-type (Wt) or TLR4$^{\Delta Cx3cr1}$ P11 mice ($n = 3$ per experimental group); (**H**) representative confocal micrographs of Mbp immunostaining in whole-brain midsagittal sections obtained from a mouse model of NEC induced in oligodendrocyte lineage reporter Pdgfrα^{GFP} transgenic P11 mice or from breastfed controls. Scale bars, 50 μm (inset). Quantification in (**I**) ($n = 4$ per experimental group). Samples were obtained from three independent experiments with at least three to four animals per experimental condition. Image analysis and quantification were performed within the indicated region of interest (ROI) obtained from midsagittal whole-brain sections using the FIJI software. Statistical significance was determined by one-way analysis of variance (ANOVA), followed by post hoc Dunnett's multiple comparisons test (E to G) and by two-tailed Student's *t* test (I).

Tlr4 by quantitative reverse transcription polymerase chain reaction (qRT-PCR) is reduced in the brains of $TLR4^{\Delta Cx3cr1}$ mice (fig. S5, A and B), and the LPS-induced expression of *Il-1*β in the brains of $TLR4^{\Delta Cx3cr1}$ mice is significantly reduced ($P < 0.01$) as compared with wild-type mice (fig. S5C). $TLR4^{\Delta Cx3cr1}$ mice were significantly protected ($P < 0.0001$) from NEC-associated brain injury, as revealed by reduced Iba-1 expression (Fig. 2, B and E), reduced DHE staining (Fig. 2, C and F) and intact pattern of myelination (Fig. 2D and quantified in Fig. 2G) compared to the wild-type mice. Together, these findings indicate that, in our animal model, NEC-associated loss of myelin requires TLR4-mediated microglial activation and results in ROS generation. We therefore next sought to determine the ligands released from the intestine that could initiate this neuroinflammatory pathway in the host and then to counteract these processes to prevent NEC-associated brain injury.

HMGB1 release from the intestinal epithelium leads to NEC-induced brain injury

To further understand the pathways leading to NEC-induced microglial activation and impaired myelination, we next focused on the intestinal-derived TLR4 ligand HMGB1 (*32, 34*), which is released from the injured intestine during mouse and human NEC (*35*). NEC was induced in wild-type mice and in mice lacking HMGB1 within the intestinal epithelium ($HMGB1^{\Delta IEC}$), which we have previously generated and which displayed significantly lower amounts of HMGB1 in the circulation compared to wild-type controls when exposed to the experimental NEC (*35*). After NEC induction, $HMGB1^{\Delta IEC}$ mice showed significantly ($P < 0.0001$) reduced microglial activation (Fig. 3A and quantified in Fig. 3D) and reduced DHE staining (Fig. 3B and quantified in Fig. 3E) and preserved Mbp expression (Fig. 3C and quantified in Fig. 3F) as compared to wild-type mouse model of NEC, confirming a role for intestinal epithelium-derived HMGB1 in the induction of the neuropathology of NEC. The importance of circulating HMGB1 in the pathogenesis of NEC-associated brain injury was further supported by the finding that the administration of intranasal anti-HMGB1 antibody to a wild-type mouse model of NEC resulted in reduced microglial activation [determined by reduced expression of Iba-1 (Fig. 3A and quantified in Fig. 3D) and by reduced DHE staining (Fig. 3B and quantified in Fig. 3E)], within the hippocampus and the periventricular region. Furthermore, Mbp expression was preserved in mice that received intranasal anti-HMGB1 [4 μg/g once a day (qd) for 4 days] as compared to mice that received nonspecific intranasal immunoglobulin G (IgG; 25 μg/g qd for 4 days) while exposed to NEC (Fig. 3C and quantified in Fig. 3F). In addition, as compared with saline-injected controls [50 μl intraperitoneal (ip) qd for 4 days], the injection of wild-type 7-day-old mice with recombinant HMGB1 [rHMGB1; 1 mg/kg (ip) qd for 4 days] resulted in increased expression of Iba-1 (Fig. 3G and quantified in Fig. 3J), accumulation of ROS within the hippocampus (Fig. 3H and quantified in Fig. 3K), and decreased Mbp expression (Fig. 3I and quantified in Fig. 3L) in an appearance resembling those seen after NEC induction. All parameters were determined on the last day of the experimental NEC model at P11 and 24 hours after the last administration of anti-HMGB1 or rHMGB1. Further supporting the role of HMGB1 in the human condition, circulating levels of HMGB1 were increased in serum obtained from infants diagnosed with NEC as compared to controls (fig. S6). As an additional control, we exposed wild-type mice to the brief hypoxia treatment used in the NEC model and found that there was no effect on ROS generation (fig. S7A and quantified in fig. S7B) or on microglial activation (fig. S7C and quantified in fig. S7D) within the mouse brain, thus reducing the possibility that the changes were due to hypoxia alone. Rather, these findings showed that brain injury in experimental NEC was associated with microglial activation and myelination impairment that might be, in part, due to the release of the TLR4 agonist HMGB1 from the inflamed intestine. We therefore next sought to prevent the development of NEC-associated brain injury using a dendrimer-based approach to specifically target and attenuate the activated microglia.

Orally administered dendrimer-based antioxidant reverses NEC-induced brain injury in mice

Given that the development of NEC-associated brain injury requires microglial TLR4 activation and ROS accumulation, we next evaluated the potential ability of a dendrimer nanoparticle coupled with the antioxidant *N*-acetyl-L-cysteine (D-NAC) to attenuate these effects. On the basis of our previous observation that intravenously administered dendrimers localize in activated microglia in experimental neuroinflammation (*36, 37*), we next administered D-NAC orally 48 hours after the initiation of experimental NEC in mice. Littermate breastfed mice were used as controls. In proof-of-concept studies shown in fig. S8, the administration of fluorescent Cy5-labeled dendrimers (D-Cy5) in the mouse model of NEC resulted in the accumulation of Cy5 fluorescence in the periventricular and hippocampus areas of the brain, consistent with the site of microglial activation and ROS accumulation. D-NAC administration resulted in a significant ($P < 0.001$) reduction in ROS accumulation (Fig. 4, A and B). Furthermore, D-NAC administration reduced microglial activation (Fig. 4, C and D) and prevented the decrease of Mbp expression (Fig. 4, E and F) and the loss of OPCs (Fig. 4, G and H), which were not different from the amount detected in the control group. In addition, D-NAC administration prevented the NEC-induced depletion of the intracellular antioxidant glutathione (Fig. 4I) and the oxidative damage to intracellular proteins [determined by the quantification of 3-nitrotyrosine levels (Fig. 4J)], which are well-known markers of oxidative stress in the brain (*37*). The effects on redox indicators were not observed with administration of free NAC, at the same dose, consistent with the low bioavailability of free NAC due to protein binding of its –SH groups (*38*). Moreover, the oral administration of D-NAC prevented the neurocognitive impairments observed in mice subjected to NEC, as demonstrated by the performance on the Y-maze (Fig. 4K, spatial working memory) and novel object recognition memory (Fig. 4L) tests. D-NAC administration did not prevent the intestinal pathology, as demonstrated in fig. S9, supporting the observation that the neuroprotective effects of D-NAC was mediated by the central nervous system, rather than through the simple attenuation of the gut pathology.

In the final series of studies, we sought to determine whether the neuropathology observed in experimental NEC and the preventive properties of D-NAC were restricted to the early stages of the disease process or whether they extended to later points as well. To do so, we evaluated the myelination profile of mice that had been exposed to experimental NEC in the presence or absence of D-NAC at 60 days from the initial intestinal injury (age P72). As shown in Fig. 5 (A and B), the expression of Mbp in whole-brain sagittal sections of these older mice that had NEC as newborns was still significantly decreased ($P < 0.0001$), even at this later time point. Mice exposed to NEC that had received D-NAC early in life displayed

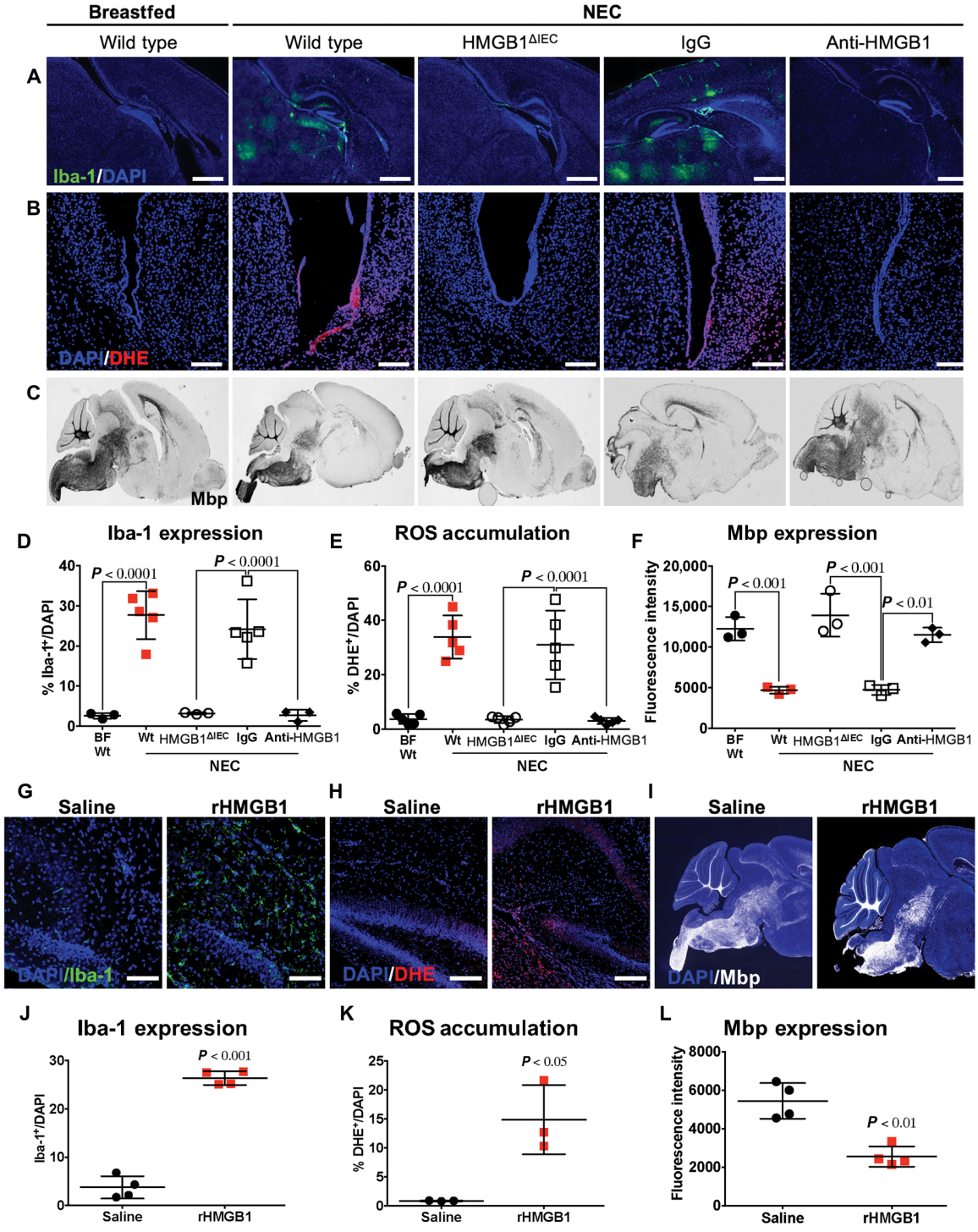

Fig. 3. HMGB1 release from the intestinal epithelium leads to NEC-induced brain injury. Representative micrographs from (**A**) hippocampus and periventricular regions, (**B**) periventricular region, and (**C**) whole-brain midsagittal section in a mouse model of NEC at P11 (stained as indicated) that were either wild type, lacking HMGB1 within the intestinal epithelium (HMGB1$^{\Delta IEC}$), or received intranasal anti-HMGB1–neutralizing or intranasal nonspecific IgG. Scale bars, 100 μm (A) and 50 μm (B). (**D** to **F**) Quantification of the indicated cells within the ROI of the hippocampus and periventricular region in the indicated group corresponding to (A) to (C) [BF, $n = 3$; NEC, $n = 5$ (Wt), $n = 3$ (HMGB1$^{\Delta IEC}$), $n = 5$ (IgG), and $n = 3$ (anti-HMGB1)]. (**G** to **I**) Representative confocal micrographs of the indicated stain in midsagittal brain sections from wild-type mice that received an intraperitoneal injection of either rHMGB1 or saline. Scale bars, 50 μm. In (I), midbrain, cerebellum, and brainstem are shown. (**J** to **L**) Quantification of the indicated cell within the ROI (hippocampus and periventricular region) in the indicated group corresponding to (G) and (H) (saline, $n = 3$; rHMGB1, $n = 4$). Samples from three to four animals were analyzed from three independent experiments. Image analysis and quantification were performed within the indicated ROI obtained from midsagittal whole-brain sections using the FIJI software. Statistical significance was determined by one-way ANOVA, followed by post hoc Dunnett's multiple comparisons test (D to F) and two-tailed Student's *t* test (J to L).

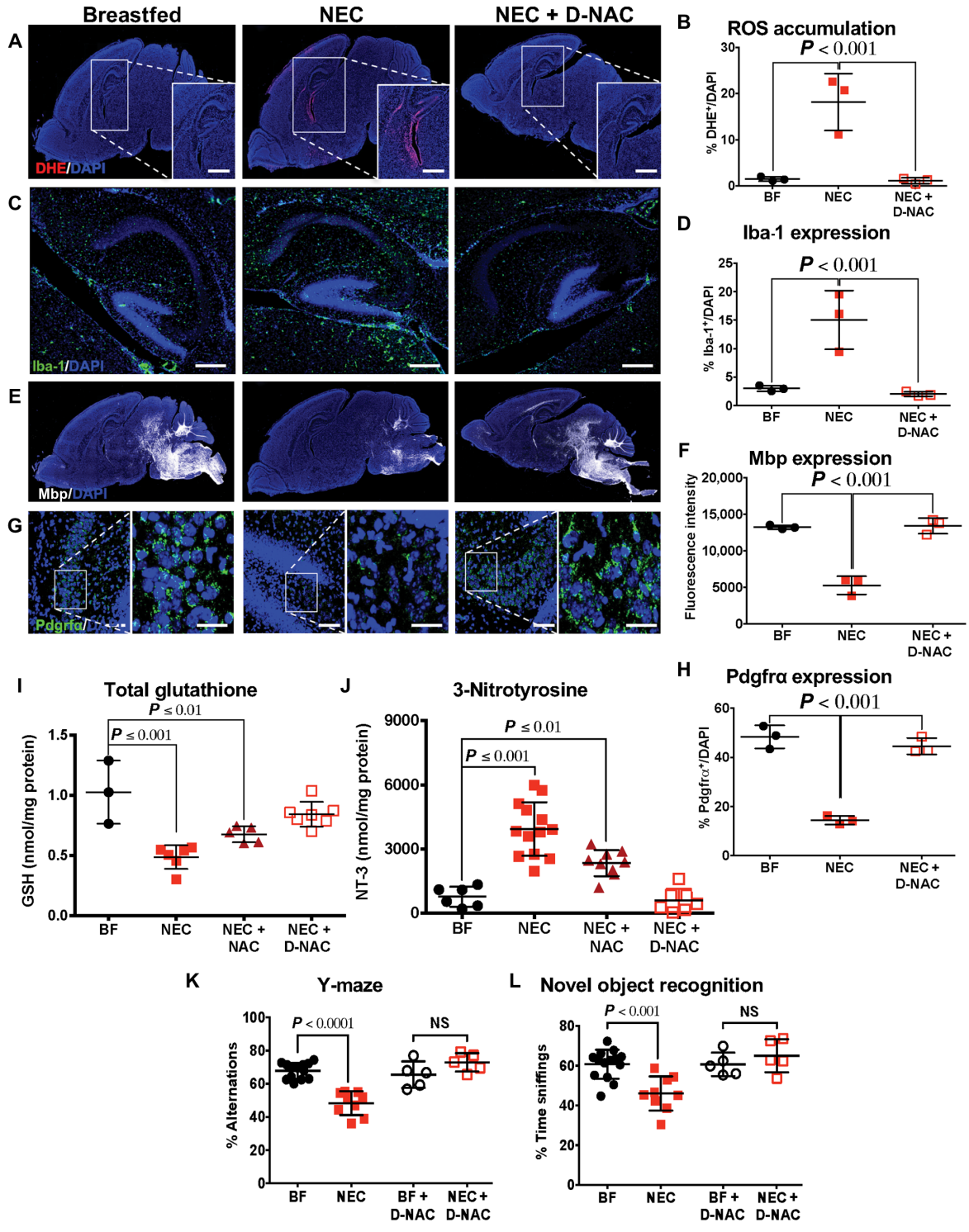

Fig. 4. Orally administered dendrimer-based antioxidant reverses NEC-induced brain injury. (**A**, **C**, **E**, and **G**) Representative micrographs showing brain sections from a mouse model of NEC in newborn mice (P11) treated or untreated with D-NAC and from breastfed controls stained as indicted and quantified in (**B**), (**D**), (**F**), and (**H**), respectively ($n = 3$ per experimental group). Scale bars, 100, 50, and 100 μm (A, C, and G, respectively) and 20 μm (inset). (**I** and **J**) Total amount of glutathione (GSH) (BF, $n = 3$; NEC, $n = 6$; NEC + NAC, $n = 5$; and NEC + D-NAC, $n = 7$) and 3-nitrotyrosine (NT-3) (BF, $n = 6$; NEC, $n = 13$; NEC + NAC, $n = 9$; and NEC + D-NAC, $n = 7$) within the hippocampus and periventricular region. All samples were obtained at the end of the NEC protocol (P11). Image analysis and quantification were performed in midsagittal whole-brain sections as described in Materials and Methods. Statistical significance was determined by one-way ANOVA, followed by post hoc Dunnett's multiple comparisons test. (**K** and **L**) Effects of D-NAC on neurocognitive testing in (K) Y-maze (BF, $n = 13$; NEC, $n = 9$; BF + D-NAC, $n = 5$; and NEC + D-NAC, $n = 5$) and in (L) novel object recognition (BF, $n = 14$; NEC, $n = 9$; BF + D-NAC, $n = 5$; NEC + D-NAC, $n = 5$) analyzed by one-way ANOVA and post hoc Tukey's test. Three independent experiments were performed with at least three mice per experimental group per experiment.

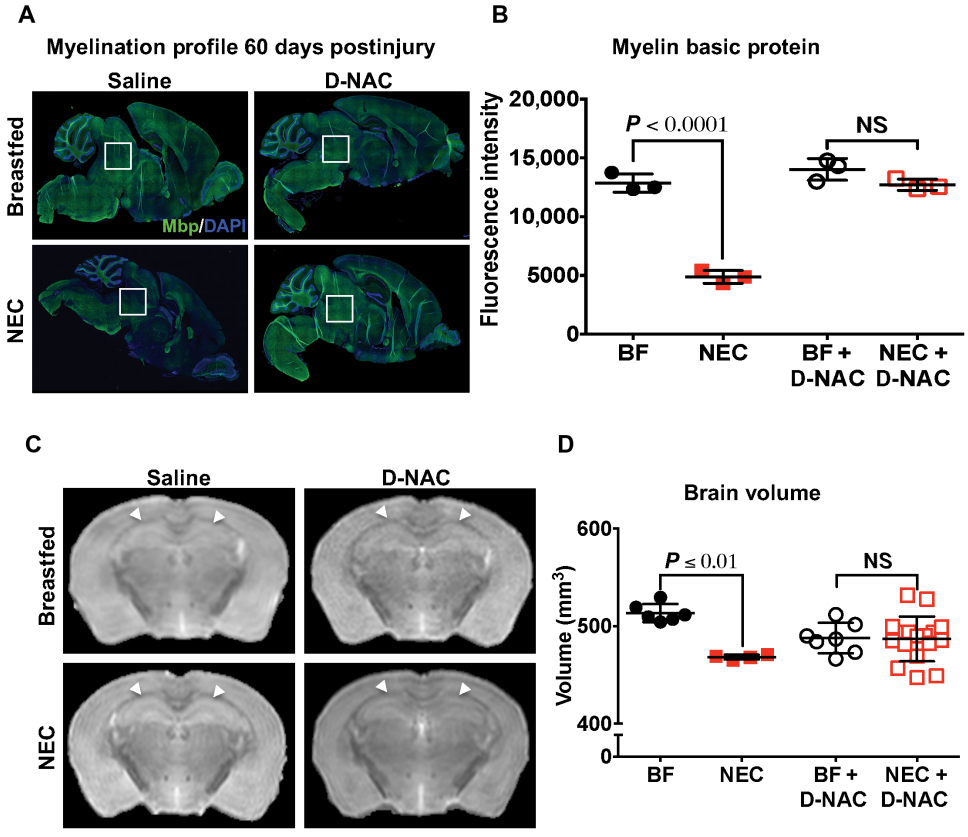

Fig. 5. D-NAC administration in early life induces long-term protection from NEC-associated myelin loss. (**A**) Micrographs showing the long-term effects (60 days after injury; P72) of D-NAC administration in a mouse model of NEC that received either saline of NAC in the newborn period stained for Mbp. (**B**) Quantification of Mbp expression ($n = 3$ per experimental condition). (**C**) Representative coronal T2-weighted images from 120-day-old (P120) mice; arrowheads indicate the corpus callosum. (**D**) Volumetric analysis of T2-weighted brain images from P120 mice (BF, $n = 6$; NEC, $n = 4$; BF + D-NAC, $n = 7$; NEC + D-NAC, $n = 17$). Two independent experiments were performed with at least three mice per experimental group per experiment. Statistical significance was determined by one-way ANOVA, followed by post hoc Tukey's multiple comparisons test.

comparable levels of Mbp expression as the age-matched breastfed controls. Brain volume, assessed by MRI in young adult mice (age P120; Fig. 5, C and D), was found to display similar findings as those observed with Mbp expression. Together, these findings reveal that NEC-associated brain injury could be durably averted through the oral administration of a dendrimer-coupled antioxidant, preventing the deleterious effects of TLR4-mediated microglial activation and ROS release.

DISCUSSION

One of the leading causes of long-term morbidity in premature infants with NEC is the development of severe neurocognitive injury, which is both more severe and more persistent than the neurocognitive injury that can develop in premature infants without NEC (*12, 13*), suggesting that a link exists between intestinal injury and toxicity to the premature brain. In the current study, we have used a mouse model of NEC to understand the mechanisms leading to the development of NEC-associated brain injury. Our mouse model bears strong similarities with clinical NEC-associated brain injury in humans, including the disruption of the normal myelination process of the midbrain, hippocampus, and subcortical regions and the subsequent development of substantial cognitive impairments as mice become older. Using this animal model, we now show that NEC-associated brain injury stems from TLR4-induced microglial activation and OPC loss, which can be inhibited via strategies that limit the downstream effects of this signaling cascade.

In seeking to prevent the deleterious effects of NEC on the newborn brain, we showed that the onset of NEC-associated brain injury in mice was associated with the accumulation of ROS mostly within the regions in which the myelination deficit was most evident (hippocampus, midbrain, and corpus callosum). The accumulation of ROS could directly affect OPCs (*39*) or directly activate microglia (*40*) or could damage the blood-brain barrier directly (*40, 41*), all of which could exacerbate the degree of brain injury in the presence of NEC. Previous studies have shown that nitrosative and oxidative stress can activate microglia in the pathogenesis of periventricular leukomalacia—a condition that affects premature infants—resulting in the arrested maturation of premyelinating oligodendrocytes (*42, 43*), suggesting similarities with our experimental model of NEC. It is noteworthy that the expression of Iba-1 was higher in the cerebellum than in other parts of the brain, although no alterations in motor function between groups were evident. On the other hand, elevated expression of Iba-1 in the hypothalamic and periventricular regions was found along with impaired cognition. The oral administration of a dendrimer-based antioxidant therapy (D-NAC) reversed the oxidant injury and prevented dysmyelination and the subsequent cognitive impairments observed in NEC-associated brain injury. D-NAC was effective when administered orally, suggesting that its passage through the intestinal mucosa can provide access to the injured region of the brain. The benefit of oral D-NAC administration in the current model raises the possibility of its use as a supplement to infant formula for administration to those infants at greatest risk for NEC-associated brain injury (*12–14*). Such dendrimer-based antioxidant therapy may be particularly well suited to infants with NEC, in which the developmental program of OPCs in the premature brain may be disrupted (*18*), and may be potentially characterized by low endogenous levels of superoxide dismutases (*44*), increasing their susceptibility to oxidant injury.

The findings of the current study may have implications for the surgical management of infants with NEC, by suggesting that delayed or incomplete removal of necrotic intestinal tissue could lead to the ongoing release of TLR4 agonists such as HMGB1, which could exert neurotoxic effects on the developing brain. These considerations are being explored directly in the form of a randomized

control trial that examines surgery versus abdominal drainage in the management of NEC with the endpoint of neurocognitive function at 2 years of age (NCT01029353).

We readily acknowledge that, although the current study provides an assessment of the mechanisms of NEC-associated brain injury using a clinically relevant mouse model, there are important limitations that suggest the opportunity for further study. Specifically, mouse models of NEC, which are used to perform detailed molecular studies, are performed typically in the first 1 to 2 weeks after birth, at a time during which the normal myelination process is still in a very dynamic state (*15*). It is thus possible that the loss of myelin that we now observe in the mouse model of NEC-associated brain injury and that we attribute to the observed loss of OPCs is in actuality reflective of delayed myelination, as opposed to myelin loss. Such a distinction is an important area for further study, especially when neuroprotective strategies are being considered. In addition, given the severity of the experimental model of NEC, studies designed to elucidate the effects of NEC on neurocognitive function at older ages require the exposure of young mice to a milder form of the disease (to increase survivability), which necessarily complicates the interpretation of the results. Another limitation is the small sample size of human samples and their wide range of gestational age that could potentially influence our results. Last, although the animal model of NEC is likely to be relevant to human NEC-associated brain injury, we acknowledge that other models of NEC exist, both in mice and in other animals (*22*), and it remains to be seen whether these models also show effects on the brain. It is hoped that the current study will provide a platform for other investigators in the field to share results from various models, to extend our understanding of the mechanisms of NEC-associated brain injury.

MATERIALS AND METHODS

Study design

The goals of this study were to elucidate the pathophysiology leading to the neurodevelopmental deficits that are frequently found in survivors of NEC and to identify a strategy to prevent NEC-associated brain injury. Using a preclinical experimental model that closely resembles the intestinal disease in mice, we correlated our findings with those present clinically and in necropsy brain specimens of infants with NEC. As detailed below, the experimental model and the collection and use of human tissue were approved by the appropriate regulatory committees at the Johns Hopkins University and the University of Pittsburgh. Treatment groups were randomly assigned, and all data were analyzed in a blinded fashion. Biological replicate numbers are stated with each corresponding result along with the specific statistical tests used.

Mice

C57Bl/6 and Cx3cr1$^{cre\text{-}ERT2}$ [B6.129P2(Cg)-Cx3cr1$^{tm2.1(cre/ERT2)Litt}$/WganJ stock no. 021160] were purchased from the Jackson Laboratory. Hmgb1$^{\Delta IEC}$ mice lacking HMGB1 on the intestinal epithelium were generated by our laboratory as we have previously described (*35*). Mice in which TLR4 was specifically deleted from microglial cells (TLR4$^{\Delta Cx3cr1}$) were generated in our laboratory by breeding Tlr4^{loxP} mice (*45*) with Cx3cr1$^{cre\text{-}ERT2}$ mice (the Jackson Laboratory). PDGRα reporter mice (Pdgrfα^{gfp}) expressing GFP in OPCs were generated by breeding mutant Gt(ROSA)26Sor$^{tm4(ACTB\text{-}tdTomato,\text{–}EGFP)}$ with tamoxifen-inducible B6N.Cg-Tg$^{(Pdgfra\text{-}cre/ERT)467Dbe/J}$ transgenic mice. Tamoxifen was intraperitoneally administered at 0.4 μg per mouse per day for two days, 48 hours before the study. For all strains, both male and female mice were randomized and used at the age indicated for each experiment.

Mice and induction of NEC

All experiments and procedures were approved by the Johns Hopkins University and the University of Pittsburgh Animal Care and Use committees in accordance to the Guide for the Care and Use of Laboratory Animals (8th Edition, The National Academies Press 2011). NEC was induced as we have previously described (*6, 46, 47*) in 7-day-old mouse pups by gavage feeding (five times per day for 4 days) of formula [Similac Advance infant formula (Abbott Nutrition) and Esbilac canine milk replacer (PetAg) at a ratio of 2:1] supplemented with enteric bacteria that were isolated from an infant with NEC (bacterial composition is presented in table S1). In control experiments, NEC was induced under the same conditions except that mice were administered bacteria from the stool of a healthy infant as opposed to an infant with NEC (bacterial composition is presented in table S2). Mice were exposed to brief hypoxia (5% O_2, 95% N_2 for 10 min twice daily) for 4 days. All animals were euthanized on P11, except in long-term studies (P72 and P120). This experimental protocol using bacteria isolated from an infant with NEC leads to patchy necrosis of the ileum and up-regulation of inflammatory cytokines, which resemble the pathologic findings of the human condition (*1, 6, 23*). Breastfed control animals were kept with the dam until the time of euthanasia. Intranasal administration of anti-HMGB1 (4 μg/g qd for 4 days) and isotype control rat IgG (25 μg/g qd for 4 days) was performed under inhalation isoflurane anesthesia. Antibodies were dissolved in 50 μl of saline and administered once a day during the NEC model starting the first day of NEC induction.

Preparation and administration of D-Cy5 and D-NAC conjugates

The synthesis and characterization of the D-Cy5 and D-NAC were performed according to our prior studies (*48*). Briefly, bifunctional dendrimers with desired amount of amines modified on the surface of hydroxyl dendrimers were prepared by adding hydroxy functionalized ethylenediamine core G4-OH (generation four polyamidoamine dendrimer) to a dimethylformamide (DMF) solution of Fmoc-GABA-OH [4-(Fmoc-amino) butyric acid] that was preactivated with PyBOP [(benzotriazol-1-yloxy) tripyrrolidinophosphonium hexafluorophosphate]. The reaction mixture was stirred at room temperature for 24 hours in the presence of DIEA (*N*,*N*′-diisopropylethylamine). Next, Fmoc was deprotected in a piperidine: DMF (2:8) solution to allow free amines being exposed on the surface of bifunctional dendrimers. The reaction mixture was then extensively dialyzed against DMF (membrane size cutoff = 2.0 kDa) to remove free Fmoc.

To label bifunctional dendrimers with Cy5-NHS ester, bifunctional dendrimers with free three to four amines on the surface were reacted with Cy5-NHS under borate buffer (pH 8.2), after extensive dialysis (membrane size cutoff = 2.0 kDa) and size exclusion chromatography to remove unreacted Cy5-NHS. The final D-Cy5 conjugates contain 5% Cy5 on mass base.

To prepare D-NAC, bifunctional dendrimers with 15 to 20 free amines on the surface were reacted with SPDP [*N*-Succinimidyl-3-(2-pyridyldithio)-propionate] in DMF for 8 hours on ice. NAC in

dimethyl sulfoxide was then added to the reaction mixture and was stirred overnight. The reaction mixture was dialyzed against DMF (membrane size cutoff = 2.0 kDa), followed with water for 2 hours to obtain pure D-NAC conjugates. NAC-coupled dendrimers (100 mg/kg qd for 2 days) were administered orally after 48 hours of starting NEC model. Both D-Cy5 and D-NAC are stable in plasma (37°C) (*49*), whereas D-NAC administration results in the release of free NAC readily under intracellular glutathione concentration (2 and 10 mM) within 3.5 hours (*50*).

Data presentation and statistical analysis

The data were analyzed using two-tailed Student's *t* test or ANOVA, followed by post hoc Dunnett's or Tukey's multiple comparisons tests using GraphPad Prism 7 software (GraphPad). Statistical significance was set at a P value of <0.05. All quantitative data are presented as means ± SD. All experiments were performed at least in triplicate, with at least three pups per group for experimental NEC. Raw data are presented in data file S1.

SUPPLEMENTARY MATERIALS

www.sciencetranslationalmedicine.org/cgi/content/full/10/471/eaan0237/DC1

Methods

Fig. S1. Experimental model of NEC in mice resembles the human intestinal disease observed in premature infants.

Fig. S2. Histological examination reveals comparable features of brain development between infants with and without NEC.

Fig. S3. Effect of the hypoxia component of the experimental NEC protocol (5% O_2, 10 min twice a day for 4 days) on cerebral myelination and brain volume.

Fig. S4. Effect of the enteric bacteria component of experimental NEC protocol on microglial activation, accumulation of ROS, and cerebral myelination.

Fig. S5. Generation of microglia-specific TLR4 knockout mice.

Fig. S6. NEC is characterized by increased circulating levels of HMGB1 in human serum.

Fig. S7. Effect of the hypoxia component of the NEC protocol on ROS accumulation and microglial activation.

Fig. S8. Dendrimer distribution within the brain after oral administration to mice with and without experimental NEC.

Fig. S9. Oral administration of D-NAC–coupled dendrimers after 48 hours of experimental NEC does not prevent the development of the intestinal disease.

Table S1. Bacterial (genus) composition found in the stool of an infant with NEC used to induce NEC in mice.

Table S2. Bacterial (genus) composition found in the stool of a healthy infant used as control in mice.

Table S3. List of primers used for qRT-PCR.

Table S4. Human brain pathology specimens.

Table S5. Postconceptual age at the time of HMGB1 blood sample collection.

Data file S1. Raw data (provided as separate Word file).

REFERENCES AND NOTES

1. D. F. Niño, C. P. Sodhi, D. J. Hackam, Necrotizing enterocolitis: New insights into pathogenesis and mechanisms. *Nat. Rev. Gastroenterol. Hepatol.* **13**, 590–600 (2016).
2. J. Neu, W. A. Walker, Necrotizing enterocolitis. *N. Engl. J. Med.* **364**, 255–264 (2011).
3. B. J. Stoll, N. I. Hansen, E. F. Bell, M. C. Walsh, W. A. Carlo, S. Shankaran, A. R. Laptook, P. J. Sánchez, K. P. Van Meurs, M. Wyckoff, A. Das, E. C. Hale, M. B. Ball, N. S. Newman, K. Schibler, B. B. Poindexter, K. A. Kennedy, C. M. Cotten, K. L. Watterberg, C. T. D'Angio, S. B. DeMauro, W. E. Truog, U. Devaskar, R. D. Higgins, Eunice Kennedy Shriver National Institute of Child Health and Human Development Neonatal Research Network, Trends in care practices, morbidity, and mortality of extremely preterm neonates, 1993-2012. *JAMA* **314**, 1039–1051 (2015).
4. B. E. Hamilton, J. A. Martin, M. J. Osterman, Births: Preliminary data for 2015. *Natl. Vital Stat. Rep.* **65**, 1–15 (2016).
5. C. L. Leaphart, J. C. Cavallo, S. C. Gribar, S. Cetin, J. Li, M. F. Branca, T. D. Dubowski, C. P. Sodhi, D. J. Hackam, A critical role for TLR4 in the pathogenesis of necrotizing enterocolitis by modulating intestinal injury and repair. *J. Immunol.* **179**, 4808–4820 (2007).
6. C. E. Egan, C. P. Sodhi, M. Good, J. Lin, H. Jia, Y. Yamaguchi, P. Lu, C. Ma, M. F. Branca, S. Weyandt, W. B. Fulton, D. F. Niño, T. Prindle Jr., J. A. Ozolek, D. J. Hackam, Toll-like receptor 4–mediated lymphocyte influx induces neonatal necrotizing enterocolitis. *J. Clin. Invest.* **126**, 495–508 (2016).
7. W. Zhou, W. Li, X. H. Zheng, X. Rong, L. G. Huang, Glutamine downregulates TLR-2 and TLR-4 expression and protects intestinal tract in preterm neonatal rats with necrotizing enterocolitis. *J. Pediatr. Surg.* **49**, 1057–1063 (2014).
8. T. Jilling, D. Simon, J. Lu, F. J. Meng, D. Li, R. Schy, R. B. Thomson, A. Soliman, M. Arditi, M. S. Caplan, The roles of bacteria and TLR4 in rat and murine models of necrotizing enterocolitis. *J. Immunol.* **177**, 3273–3282 (2006).
9. D. Meng, W. Zhu, H. N. Shi, L. Lu, V. Wijendran, W. Xu, W. A. Walker, Toll-like receptor-4 in human and mouse colonic epithelium is developmentally regulated: A possible role in necrotizing enterocolitis. *Pediatr. Res.* **77**, 416–424 (2015).
10. V. Chau, R. Brant, K. J. Poskitt, E. W. Y. Tam, A. Synnes, S. P. Miller, Postnatal infection is associated with widespread abnormalities of brain development in premature newborns. *Pediatr. Res.* **71**, 274–279 (2012).
11. D. K. Shah, L. W. Doyle, P. J. Anderson, M. Bear, A. J. Daley, R. W. Hunt, T. E. Inder, Adverse neurodevelopment in preterm infants with postnatal sepsis or necrotizing enterocolitis is mediated by white matter abnormalities on magnetic resonance imaging at term. *J. Pediatr.* **153**, 170–175–175.e1 (2008).
12. R. Wadhawan, W. Oh, S. R. Hintz, M. L. Blakely, A. Das, E. F. Bell, S. Saha, A. R. Laptook, S. Shankaran, B. J. Stoll, M. C. Walsh, R. D. Higgins, NICHD Neonatal Research Network, Neurodevelopmental outcomes of extremely low birth weight infants with spontaneous intestinal perforation or surgical necrotizing enterocolitis. *J. Perinatol.* **34**, 64–70 (2014).
13. T. A. Shah, J. Meinzen-Derr, T. Gratton, J. Steichen, E. F. Donovan, K. Yolton, B. Alexander, V. Narendran, K. R. Schibler, Hospital and neurodevelopmental outcomes of extremely low-birth-weight infants with necrotizing enterocolitis and spontaneous intestinal perforation. *J. Perinatol.* **32**, 552–558 (2012).
14. B. J. Stoll, N. I. Hansen, I. Adams-Chapman, A. A. Fanaroff, S. R. Hintz, B. Vohr, R. D. Higgins, National Institute of Child Health and Human Development Neonatal Research Network, Neurodevelopmental and growth impairment among extremely low-birth-weight infants with neonatal infection. *JAMA* **292**, 2357–2365 (2004).
15. N. Salmaso, B. Jablonska, J. Scafidi, F. M. Vaccarino, V. Gallo, Neurobiology of premature brain injury. *Nat. Neurosci.* **17**, 341–346 (2014).
16. J. A. Ivacko, R. Sun, F. S. Silverstein, Hypoxic-ischemic brain injury induces an acute microglial reaction in perinatal rats. *Pediatr. Res.* **39**, 39–47 (1996).
17. H. Hagberg, C. Mallard, D. M. Ferriero, S. J. Vannucci, S. W. Levison, Z. S. Vexler, P. Gressens, The role of inflammation in perinatal brain injury. *Nat. Rev. Neurol.* **11**, 192–208 (2015).
18. S. A. Back, Cerebral white and gray matter injury in newborns: New insights into pathophysiology and management. *Clin. Perinatol.* **41**, 1–24 (2014).
19. A. A. Baburamani, V. G. Supramaniam, H. Hagberg, C. Mallard, Microglia toxicity in preterm brain injury. *Reprod. Toxicol.* **48**, 106–112 (2014).
20. S. L. Merhar, Y. Ramos, J. Meinzen-Derr, B. M. Kline-Fath, Brain magnetic resonance imaging in infants with surgical necrotizing enterocolitis or spontaneous intestinal perforation versus medical necrotizing enterocolitis. *J. Pediatr.* **164**, 410–412.e1 (2014).
21. S. H. Shin, E.-K. Kim, H. Yoo, Y. H. Choi, S. Kim, B. K. Lee, Y. H. Jung, H.-Y. Kim, H.-S. Kim, J.-H. Choi, Surgical necrotizing enterocolitis versus spontaneous intestinal perforation in white matter injury on brain magnetic resonance imaging. *Neonatology* **110**, 148–154 (2016).
22. P. Lu, C. P. Sodhi, H. Jia, S. Shaffiey, M. Good, M. F. Branca, D. J. Hackam, Animal models of gastrointestinal and liver diseases. Animal models of necrotizing enterocolitis: Pathophysiology, translational relevance, and challenges. *Am. J. Physiol. Gastrointest. Liver Physiol.* **306**, G917–G928 (2014).
23. A. Afrazi, M. F. Branca, C. P. Sodhi, M. Good, Y. Yamaguchi, C. E. Egan, P. Lu, H. Jia, S. Shaffiey, J. Lin, C. Ma, G. Vincent, T. Prindle Jr., S. Weyandt, M. D. Neal, J. A. Ozolek, J. Wiersch, M. Tschurtschenthaler, C. Shiota, G. K. Gittes, T. R. Billiar, K. Mollen, A. Kaser, R. Blumberg, D. J. Hackam, Toll-like receptor 4-mediated endoplasmic reticulum stress in intestinal crypts induces necrotizing enterocolitis. *J. Biol. Chem.* **289**, 9584–9599 (2014).
24. M. D. Neal, C. P. Sodhi, M. Dyer, B. T. Craig, M. Good, H. Jia, I. Yazji, A. Afrazi, W. M. Richardson, D. Beer-Stolz, C. Ma, T. Prindle, Z. Grant, M. F. Branca, J. Ozolek, D. J. Hackam, A critical role for TLR4 induction of autophagy in the regulation of enterocyte migration and the pathogenesis of necrotizing enterocolitis. *J. Immunol.* **190**, 3541–3551 (2013).
25. K. L. West, N. D. Kelm, R. P. Carson, M. D. Does, A revised model for estimating g-ratio from MRI. *Neuroimage* **125**, 1155–1158 (2016).
26. K. L. West, N. D. Kelm, R. P. Carson, M. D. Does, Quantitative analysis of mouse corpus callosum from electron microscopy images. *Data Brief* **5**, 124–128 (2015).
27. M. Aggarwal, S. Mori, T. Shimogori, S. Blackshaw, J. Zhang, Three-dimensional diffusion tensor microimaging for anatomical characterization of the mouse brain. *Magn. Reson. Med.* **64**, 249–261 (2010).
28. J. C. Silbereis, E. J. Huang, S. A. Back, D. H. Rowitch, Towards improved animal models of neonatal white matter injury associated with cerebral palsy. *Dis. Model. Mech.* **3**, 678–688 (2010).
29. M. V. Pletnikov, Y. Ayhan, O. Nikolskaia, Y. Xu, M. V. Ovanesov, H. Huang, S. Mori, T. H. Moran, C. A. Ross, Inducible expression of mutant human DISC1 in mice is associated

with brain and behavioral abnormalities reminiscent of schizophrenia. *Mol. Psychiatry* **13**, 173–186 (2008).
30. C. R. Martin, O. Dammann, E. N. Allred, S. Patel, T. M. O'Shea, K. C. K. Kuban, A. Leviton, Neurodevelopment of extremely preterm infants who had necrotizing enterocolitis with or without late bacteremia. *J. Pediatr.* **157**, 751–756.e1 (2010).
31. P. Lu, C. P. Sodhi, Y. Yamaguchi, H. Jia, T. Prindle Jr., W. B. Fulton, A. Vikram, K. J. Bibby, M. J. Morowitz, D. J. Hackam, Intestinal epithelial toll-like receptor 4 prevents metabolic syndrome by regulating interactions between microbes and intestinal epithelial cells in mice. *Mucosal Immunol.* **11**, 727–740 (2018).
32. S. Kim, S. Y. Kim, J. P. Pribis, M. Lotze, K. P. Mollen, R. Shapiro, P. Loughran, M. J. Scott, T. R. Billiar, Signaling of high mobility group box 1 (HMGB1) through toll-like receptor 4 in macrophages requires CD14. *Mol. Med.* **19**, 88–98 (2013).
33. M. Yu, H. Wang, A. Ding, D. T. Golenbock, E. Latz, C. J. Czura, M. J. Fenton, K. J. Tracey, H. Yang, HMGB1 signals through toll-like receptor (TLR) 4 and TLR2. *Shock* **26**, 174–179 (2006).
34. J. R. Klune, R. Dhupar, J. Cardinal, T. R. Billiar, A. Tsung, HMGB1: Endogenous danger signaling. *Mol. Med.* **14**, 476–484 (2008).
35. H. Jia, C. P. Sodhi, Y. Yamaguchi, P. Lu, L. Y. Martin, M. Good, Q. Zhou, J. Sung, W. B. Fulton, D. F. Niño, T. Prindle Jr., J. A. Ozolek, D. J. Hackam, Pulmonary epithelial TLR4 activation leads to lung injury in neonatal necrotizing enterocolitis. *J. Immunol.* **197**, 859–871 (2016).
36. E. Nance, M. Porambo, F. Zhang, M. K. Mishra, M. Buelow, R. Getzenberg, M. Johnston, R. M. Kannan, A. Fatemi, S. Kannan, Systemic dendrimer-drug treatment of ischemia-induced neonatal white matter injury. *J. Control. Release* **214**, 112–120 (2015).
37. S. Kannan, H. Dai, R. S. Navath, B. Balakrishnan, A. Jyoti, J. Janisse, R. Romero, R. M. Kannan, Dendrimer-based postnatal therapy for neuroinflammation and cerebral palsy in a rabbit model. *Sci. Transl. Med.* **4**, 130ra146 (2012).
38. B. Olsson, M. Johansson, J. Gabrielsson, P. Bolme, Pharmacokinetics and bioavailability of reduced and oxidized N-acetylcysteine. *Eur. J. Clin. Pharmacol.* **34**, 77–82 (1988).
39. S. A. Back, N. L. Luo, N. S. Borenstein, J. M. Levine, J. J. Volpe, H. C. Kinney, Late oligodendrocyte progenitors coincide with the developmental window of vulnerability for human perinatal white matter injury. *J. Neurosci.* **21**, 1302–1312 (2001).
40. M. L. Block, L. Zecca, J. S. Hong, Microglia-mediated neurotoxicity: Uncovering the molecular mechanisms. *Nat. Rev. Neurosci.* **8**, 57–69 (2007).
41. R. Moretti, J. Pansiot, D. Bettati, N. Strazielle, J. F. Ghersi-Egea, G. Damante, B. Fleiss, L. Titomanlio, P. Gressens, Blood-brain barrier dysfunction in disorders of the developing brain. *Front. Neurosci.* **9**, 40 (2015).
42. R. L. Haynes, R. D. Folkerth, F. L. Trachtenberg, J. J. Volpe, H. C. Kinney, Nitrosative stress and inducible nitric oxide synthase expression in periventricular leukomalacia. *Acta Neuropathol.* **118**, 391–399 (2009).
43. R. L. Haynes, R. D. Folkerth, R. J. Keefe, I. Sung, L. I. Swzeda, P. A. Rosenberg, J. J. Volpe, H. C. Kinney, Nitrosative and oxidative injury to premyelinating oligodendrocytes in periventricular leukomalacia. *J. Neuropathol. Exp. Neurol.* **62**, 441–450 (2003).
44. P. L. Follett, P. A. Rosenberg, J. J. Volpe, F. E. Jensen, NBQX attenuates excitotoxic injury in developing white matter. *J. Neurosci.* **20**, 9235–9241 (2000).
45. C. P. Sodhi, M. D. Neal, R. Siggers, S. Sho, C. Ma, M. F. Branca, T. Prindle Jr., A. M. Russo, A. Afrazi, M. Good, R. Brower-Sinning, B. Firek, M. J. Morowitz, J. A. Ozolek, G. K. Gittes, T. R. Billiar, D. J. Hackam, Intestinal epithelial toll-like receptor 4 regulates goblet cell development and is required for necrotizing enterocolitis in mice. *Gastroenterology* **143**, 708–718.e5 (2012).
46. M. Good, C. P. Sodhi, C. E. Egan, A. Afrazi, H. Jia, Y. Yamaguchi, P. Lu, M. F. Branca, C. Ma, T. Prindle Jr., S. Mielo, A. Pompa, Z. Hodzic, J. A. Ozolek, D. J. Hackam, Breast milk protects against the development of necrotizing enterocolitis through inhibition of toll-like receptor 4 in the intestinal epithelium via activation of the epidermal growth factor receptor. *Mucosal Immunol.* **8**, 1166–1179 (2015).
47. I. Yazji, C. P. Sodhi, E. K. Lee, M. Good, C. E. Egan, A. Afrazi, M. D. Neal, H. Jia, J. Lin, C. Ma, M. F. Branca, T. Prindle, W. M. Richardson, J. Ozolek, T. R. Billiar, D. G. Binion, M. T. Gladwin, D. J. Hackam, Endothelial TLR4 activation impairs intestinal microcirculatory perfusion in necrotizing enterocolitis via eNOS-NO-nitrite signaling. *Proc. Natl. Acad. Sci. U.S.A.* **110**, 9451–9456 (2013).
48. M. K. Mishra, C. A. Beaty, W. G. Lesniak, S. P. Kambhampati, F. Zhang, M. A. Wilson, M. E. Blue, J. C. Troncoso, S. Kannan, M. V. Johnston, W. A. Baumgartner, R. M. Kannan, Dendrimer brain uptake and targeted therapy for brain injury in a large animal model of hypothermic circulatory arrest. *ACS Nano* **8**, 2134–2147 (2014).
49. W. G. Lesniak, M. K. Mishra, A. Jyoti, B. Balakrishnan, F. Zhang, E. Nance, R. Romero, S. Kannan, R. M. Kannan, Biodistribution of fluorescently labeled PAMAM dendrimers in neonatal rabbits: Effect of neuroinflammation. *Mol. Pharm.* **10**, 4560–4571 (2013).
50. Y. E. Kurtoglu, R. S. Navath, B. Wang, S. Kannan, R. Romero, R. M. Kannan, Poly(amidoamine) dendrimer-drug conjugates with disulfide linkages for intracellular drug delivery. *Biomaterials* **30**, 2112–2121 (2009).

Acknowledgments: We thank T. CreveCoeur, E. Partan, and R. Sharma for technical assistance with the experiments described. **Funding:** D.J.H. is supported by grant nos. R01GM078238 and R01DK083752 from the NIH. **Author contributions:** D.F.N. wrote and edited the manuscript, designed, planned, and conducted experiments, and analyzed results. D.J.H. and C.P.S. wrote and edited the manuscript, planned experiments, and reviewed results. D.J.H. secured and maintained funding for the project and provided oversight and regulatory compliance. S.K., R.M.K., F.Z., S.M., M.P., and A.F. planned and designed the experiments, edited the manuscript, and reviewed results. Y.Y., L.Y.M., S.W., W.B.F., Q.Z., H.J., P.L.,T.P., F.Z., J.C., and Z.H. conducted experiments. A.G. and L.L.C. obtained human pathology specimens and reviewed results. **Competing interests:** S.K. and R.M.K. have filed a patent for the use of D-NAC in the treatment of neurological disorders (PCT/US2015/045112–Selective dendrimer delivery to brain tumors). S.K. holds equity in Ashvattha LLC and Orpheris Inc. that are focused on translational and commercialization of dendrimer drug therapies. All other authors declare that they have no competing interests. **Data and materials availability:** D-NAC can be obtained through a material transfer agreement (MTA). Purified rHMGB1 and anti-HMGB1–neutralizing antibody were used under an MTA between the Johns Hopkins University and the Feinstein Institute for Medical Research. All the data are present in the main text or in the Supplementary Materials.

Submitted 27 February 2017
Resubmitted 21 April 2018
Accepted 23 July 2018
Published 12 December 2018
10.1126/scitranslmed.aan0237

Citation: D. F. Niño, Q. Zhou, Y. Yamaguchi, L. Y. Martin, S. Wang, W. B. Fulton, H. Jia, P. Lu, T. Prindle Jr., F. Zhang, J. Crawford, Z. Hou, S. Mori, L. L. Chen, A. Guajardo, A. Fatemi, M. Pletnikov, R. M. Kannan, S. Kannan, C. P. Sodhi, D. J. Hackam, Cognitive impairments induced by necrotizing enterocolitis can be prevented by inhibiting microglial activation in mouse brain. *Sci. Transl. Med.* **10**, eaan0237 (2018).

Science Translational Medicine

Cognitive impairments induced by necrotizing enterocolitis can be prevented by inhibiting microglial activation in mouse brain

Diego F. Niño, Qinjie Zhou, Yukihiro Yamaguchi, Laura Y. Martin, Sanxia Wang, William B. Fulton, Hongpeng Jia, Peng Lu, Thomas Prindle, Jr., Fan Zhang, Joshua Crawford, Zhipeng Hou, Susumu Mori, Liam L. Chen, Andrew Guajardo, Ali Fatemi, Mikhail Pletnikov, Rangaramanujam M. Kannan, Sujatha Kannan, Chhinder P. Sodhi and David J. Hackam

Sci Transl Med **10**, eaan0237.
DOI: 10.1126/scitranslmed.aan0237

The gut-brain conNECtion

Necrotizing enterocolitis (NEC) is a gastrointestinal disorder affecting premature infants. Newborns with NEC often develop cognitive impairments. The mechanisms leading to cognitive disabilities remain unclear. Niño *et al.* show that increased oxidative stress in the brain triggered NEC-associated cognitive impairments in mice. The release of the proinflammatory molecule high-mobility group box 1 from the injured intestine activated Toll-like receptor 4 on microglial cells in the brain, resulting in accumulation of reactive oxygen species. Oral administration of microglia-targeting antioxidants prevented cognitive impairments in a mouse model of NEC. The results suggest that reducing microglial activation might be a strategy to protect patients from cognitive impairments associated with NEC.